
Nonlinear buffeting response of bridge deck using the Band Superposition approach: comparison between rheological models and convolution integrals.

Argentini, T.¹⁾, Diana, G.¹⁾, Portentos, M. ^{*1)}, Rocchi, D. ¹⁾

1) *Politecnico di Milano, Department of Mechanical Engineering, Milano, Italy*

**) presenting author, michele.portentos@polimi.it*

ABSTRACT

The nonlinear aerodynamic effects on a multi-box deck section are both numerically and experimentally investigated using the Band Superposition approach. An approach based on a rheological model approach and a convolution integral approach are compared for the simulation of high frequency unsteady forces, modulated by the low-frequency band results. The numerical model is validated against wind tunnel tests performed by means of an active turbulence generator and a multi-box deck sectional model. Finally, the linear and nonlinear approaches are compared with full-scale simulations of the numerical response of a sectional bridge to an incoming real turbulent wind.

1 INTRODUCTION

In bridges aerodynamics, the modelling of non-linearities of wind-loads on the decks is still an open issue. The *Band Superposition* approach (BS) (Diana et al., (1995, 2013); Chen and Kareem, (2001,2003); Chen et al., (2000)) is a well-established procedure to account for nonlinear aerodynamic effects, exploiting the knowledge of the static coefficients, of the flutter derivatives, and of the admittance functions, as a function of the reduced velocity and of the mean angle of attack.

The BS approach relies on the assumption that nonlinear effects acting at low frequency (LF band) are mainly induced by the large fluctuation on the instantaneous angle of attack α_{LF} , while the nonlinear effects at high frequency (HF band) may be modelled by a linearized approach around the LF band solution. In the HF band, the dependence on both the reduced velocity and the angle of attack is taken into account through a numerical model whose coefficients change in time, while for the LF band a corrected quasi-steady approach is used.

Bocciolone et al. (1992) showed the occurrence of large fluctuation of the instantaneous angle of attack caused by the high correlated low frequency components of the incoming wind. On the other hand, several experimental wind tunnel tests (e.g. Diana et al. (2013)) demonstrated the strong dependence on the bridge HF response on the LF angle of attack.

The algorithm flow-chart is reported in Figure 1, and the procedure consists of three main steps:

LF-HF threshold definition \rightarrow *LF response computation* \rightarrow *HF response computation*

The LF-HF threshold has to be defined in terms of reduced velocity V^* or reduced frequency f^* . This threshold delimits the region where the flutter derivatives and the aerodynamic admittance functions show small dependence on the reduced velocity. For the Messina bridge, the value is around $V^*=15$. The LF computation can be simulated using a nonlinear corrected quasi-steady theory (e.g. Diana et al. (1995, 2013)) or with a hysteresis loop approach (Diana et al., (2008, 2010)).

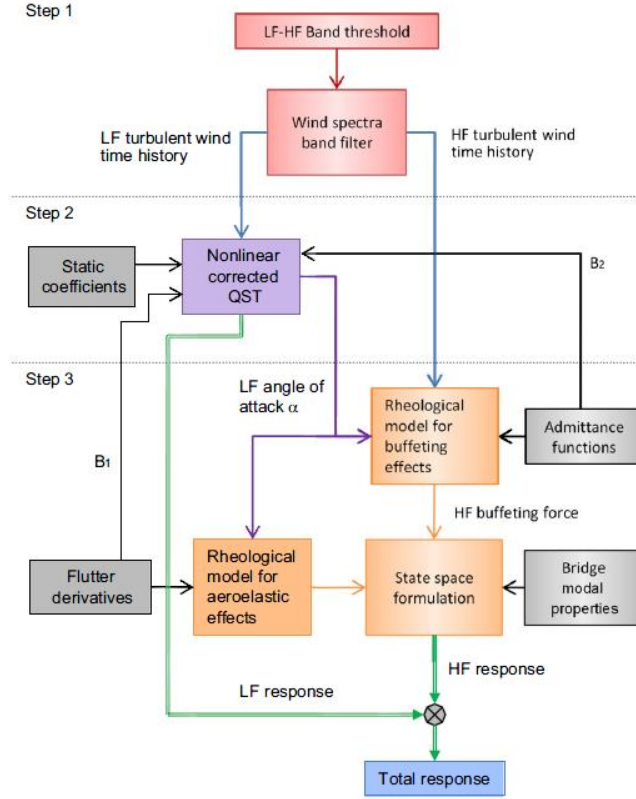


Figure 1: Band Superposition algorithm flow-chart (after Diana et al., 2013).

The HF band solution can be simulated with a rheological numerical model (Diana et al., 2013) that computes the aerodynamic forces by summing up the forces that a group of simple mechanical systems whose parameters are modulated by the instantaneous LF angle of attack. Alternatively (Chen and Kareem, 2001), the HF band forces can be simulated using a convolution integral of the impulse response functions of the corresponding aerodynamic transfer functions, as it is explained in the following section. In both cases, self-induced and buffeting forces are computed independently and their effect are summed up exploiting the superposition hypothesis.

In this paper, we present a comparison of these two numerical approaches for HF forces and their validation against experimental results obtained in wind tunnel on a section model of the Messina Bridge. The BS approach is finally used to simulate the buffeting response of a sectional model in turbulent wind and results are compared to a linear approach.

2 RHEOLOGICAL AND CONVOLUTION APPROACH

Both the rheological and the convolution approach are based on the concept of the aerodynamic force transfer function that are identified through wind tunnel tests. As an example, the self-excited aerodynamic moment induced by a torsional motion of the deck per unit of length can be expressed as:

$$M_{se}(\theta_{HF}) = \frac{1}{2} \rho V^2 B^2 \left[a_3^* - i \frac{2\pi}{V^*} a_2^* \right] \theta_{HF} = \frac{1}{2} \rho V^2 B^2 \left[T_{M\theta}(\alpha_{LF}, V^*) \right] \theta_{HF} \quad (1)$$

where a_2^* and a_3^* are the torsional flutter derivatives (Zasso (1996)), and $T_{M\theta}$ is the corresponding aerodynamic transfer function between moment coefficient and torsional displacement θ_{HF} .

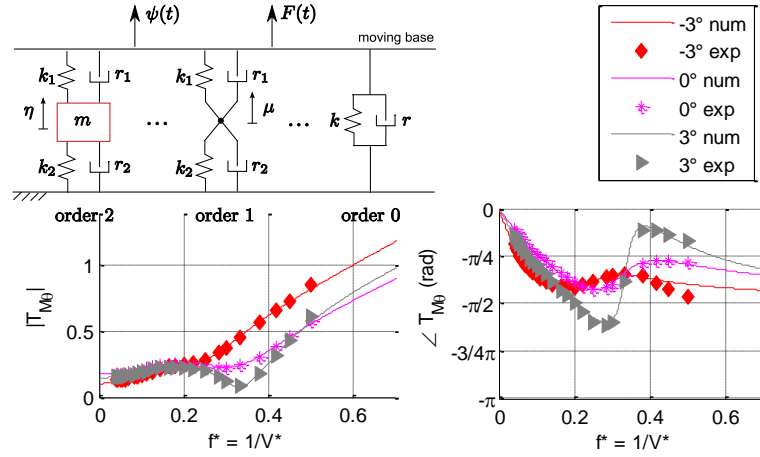


Figure 2: Scheme for rheological model and comparison of experimental and numerical transfer functions.

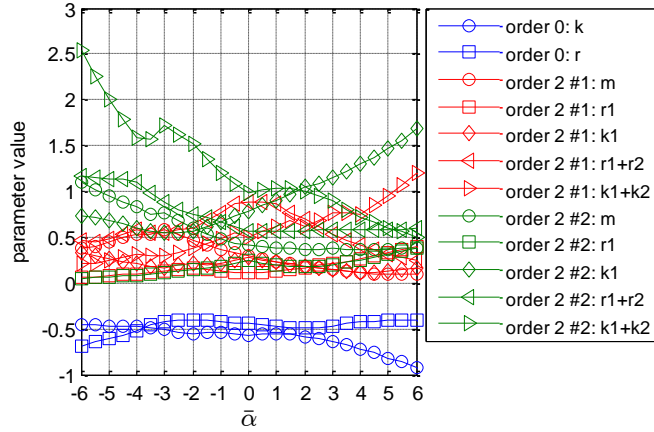


Figure 3: Parameters of the rheological model as a function of the mean angle of attack.

2.1 Rheological approach

The rheological model approach consists in defining a set of linear oscillators that are able to reproduce the aerodynamic transfer functions (for self-excited and buffeting forces), see Figure 2. Since the aerodynamic transfer functions vary according to the mean angle of α , it is required to identify different sets of mechanical parameters (see Figure 3). Therefore, mass, springs, dampers change their value according to the mean angle of attack that in the BS approach is determined by the slowly varying α_{LF} .

For every force component (Drag, Lift, and Moment) and for every input (displacements y , z , θ or turbulent wind velocity components w and u) a different rheological model needs to be identified (15 in total). Each transfer function requires, for the simulation in time domain, about 5 additional aerodynamic states (dofs of the model). Therefore, it is clear that this approach is computationally demanding, especially if it is applied to a full-bridge with multiple sections (which are in general set every 5-10m span).

2.2 Convolution approach

The convolution approach consists in simulating the aerodynamic forces by means of the convolution integral, assuming the HF input as a train of modulated impulses. Starting from the aerodynamic transfer function it is possible to extract the impulse response function of each force.

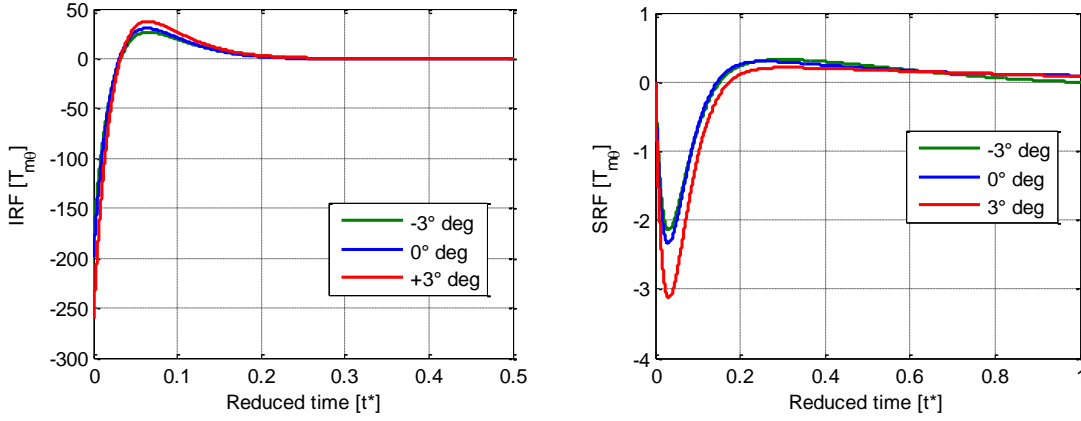


Figure 4: Impulse Response Functions and corresponding Step Response Functions for three different mean angles of attack (to be compared with Figure 2).

As an example, if we still consider the transfer function $T_{M\theta}$ and if we compute the Inverse Fourier Transform of it, we obtain the impulse response function, in time domain, of the moment coefficient resulting to an impulse input θ_{HF} . In this case, the numerical transfer function obtained by the rheological models is used, in order to allow for a direct comparison of the two approaches. Figure 4 reports the Impulse Response Functions and corresponding Step Response Functions for three different mean angles of attack.

Thus, the time evolution of the force M due to a HF variable θ_{HF} can be obtained as follow:

$$\begin{aligned}
 M_{se}(t^*) &= \frac{1}{2} \rho V^2 B^2 \left\{ IFT \left[T_{M\theta}(\alpha_{LF}, V^*) \right] \otimes \theta_{HF}(t) \right\} \\
 &= \frac{1}{2} \rho V^2 B^2 \left\{ \int_0^{t^*} I_{M\theta, \alpha_{LF}}(t^* - \tau) \theta_{HF}(\tau) d\tau \right\}
 \end{aligned} \tag{2}$$

where $I_{M\theta, \alpha_{LF}}$ is the impulse response function that depends on the instantaneous LF varying angle of attack. It should be note that, since we starts from an non-dimensional definition of the aerodynamic variables (in terms of V^* or f^*) the integration defined in Eq.(2) is still in terms of non-dimensional time $t^* = tV/B$.

As shown in Figure 4 the impulse responses of the aerodynamic functions have a very fast dynamics, which require a very small time resolution to be properly defined. To overcome this limit, for linear systems, the convolution of the impulse response is generally replaced with the convolution of the step response (passing through an integration by parts), which allows for less fine time resolution (see Figure 5). However, the idea of enforcing the convolution integral with the step response function, has some analytical drawbacks and cannot be properly applied when a variation of the parameters occurs. This is due to the fact that step response (S) and impulse response (I) are related by a time derivative:

$$I(\alpha_{LF}(t), t) = \frac{dS(\alpha_{LF}, t)}{dt} = \frac{\partial S(\alpha_{LF}, t)}{\partial t} + \frac{\partial S(\alpha_{LF}, t)}{\partial \alpha_{LF}} \dot{\alpha}_{LF} \tag{3}$$

Therefore the integration by parts should account for an additional term (derivative w.r.t. α) which is difficult to handle, and that is not present if a constant angle of attack is considered. As a consequence the convolution approach has to be done using IRFs, which are computationally demanding in the sense that they require small time steps (for the considered test case, a reduced time step of $1e-4$ is used).

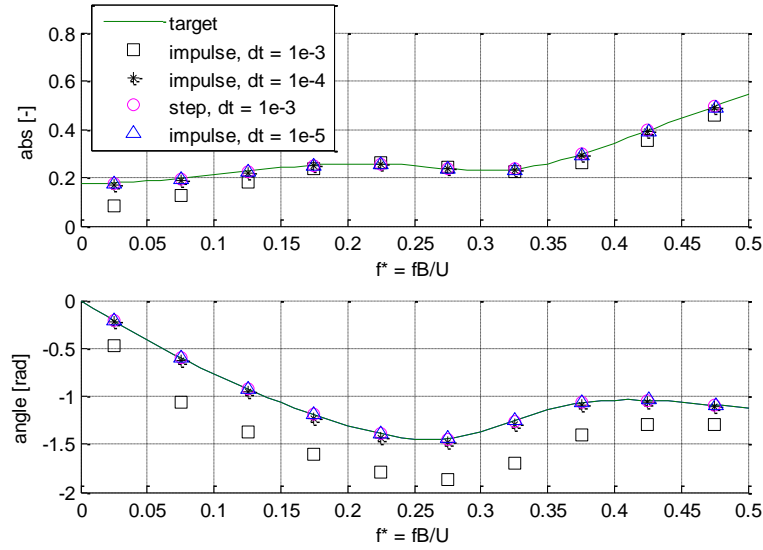


Figure 5: Effect of time step on the simulation of the aerodynamic transfer function $T_{M\theta}$: target and simulated with different methods (impulse/step) and time resolution (dt).



Figure 6: Experimental test rig

3 FORCE MODEL VALIDATION

To validate the model of the aerodynamic forces, a series of wind tunnel test were performed at the Politecnico di Milano wind tunnel on a deck sectional model representing a bridge multi-box deck shape, already investigated during the Messina Bridge design. The sectional model is 4 m long and has a chord of 1.33 m; the central dynamometric part is 1.33 m wide. The system is equipped with three hydraulic actuators and they allow to move the deck at various mean angle (-6:+6) with a constant motion amplitude. An active turbulence generator, made by horizontal airfoils 6 m long and harmonically driven, which is able to introduce high correlated vertical turbulences with specific frequencies, completes the test rig (see Fig. 6). The setup is able to reproduce the BS situation with a LF component plus a HF component.

In Figures 7 – 8, we present the results obtained by the linear and non-linear models concerning the HF self-excited aerodynamic moment induced by a torsional motion θ_{HF} (at 2.4 Hz) in presence of a variation of the instantaneous angle of attack induced by a LF fluctuation of the vertical wind component (w_{LF} at 0.25 Hz). Table 1 reports magnitude and phase of the most relevant harmonics. Both rheological and convolution approaches simulate accurately both in terms of magnitude and phase the nonlinear dependence of HF forces upon LF fluctuation of the angle of attack. These results hold also for lift and drag, and for different HF inputs (e.g. vertical displacement z or turbulence w).

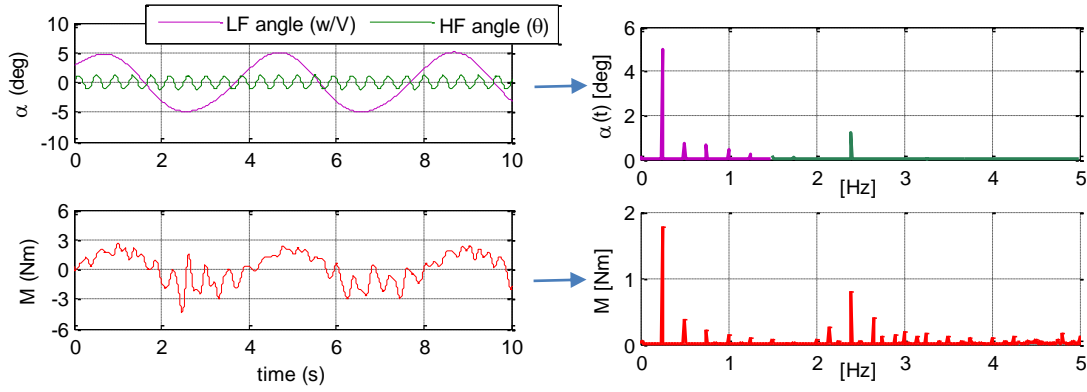


Figure 7: Forced motion tests. Left: Time histories of LF+HF inputs and corresponding aerodynamic moment. Right: Spectra

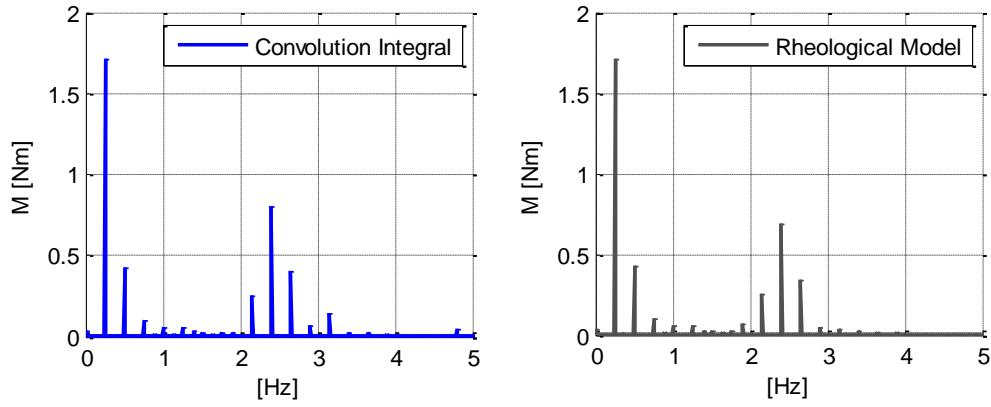


Figure 8: Numerical outputs of forced motion tests: convolution integral of IRF (left) and rheological model (right)(to be compared with Figure 7 and summarized in Tab 1).

Table 1: Comparison of main harmonics of the aerodynamic moment in terms of magnitude and phase: experimental vs. different numerical schemes

Frequency [Hz]	0.25	0.5	2.15	2.4	2.65
Experimental (mod)	1.78	0.38	0.27	0.80	0.39
(phase)	-23°	224°	217°	-65°	65°
Linear (mod)	1.84	--	--	0.7	--
(phase)	-28°	--	--	-74°	--
Rheological (mod)	1.7	0.43	0.26	0.68	0.34
(phase)	-27°	216°	218°	-68°	69°
Convolution (mod)	1.7	0.43	0.25	0.80	0.41
(phase)	-27°	216°	206°	-78	57°

4 NUMERICAL BUFFETING RESPONSE

Numerical simulations of the deck response under the action of a turbulent wind are performed using the linear and the BS approach (both Convolution and Rheological model). Full-scale simulations are performed considering a suspended deck sectional model (Table 2) run over by a fully turbulent wind completely correlated along the deck length ($I_u = 13.8\%$, $I_w = 6.9\%$, see Figure 9).

Considering a test case with a mean wind speed of 60 m/s, results are summarized in Table 3 and Figure 10. Table 3 reports the standard deviations and the maxima of the time histories of the horizontal (y), vertical (z), and torsional (θ) displacements of the deck: we can notice that the convolution and the rheological approaches give similar results. Figure 10 shows a comparison of the power spectral densities of the response. As it can be seen, when a nonlinear approach is applied, the introduction of super/sub-harmonics in the forces results in a wider band spectral content with respect to the linear approach.

Table 2: Modal parameters of the bridge

Mode	Natural frequency (Hz)	Modal mass	Damping coefficient	Mode shape y-component	Mode shape z-component	Mode shape θ -component
1	0.0927	6.7e3 kg/m	0.01	1	0	0
2	0.1977	6.7e3 kg/m	0.01	0	1	0
3	0.2418	4.7e6 kg m ² /m	0.01	0	0	1

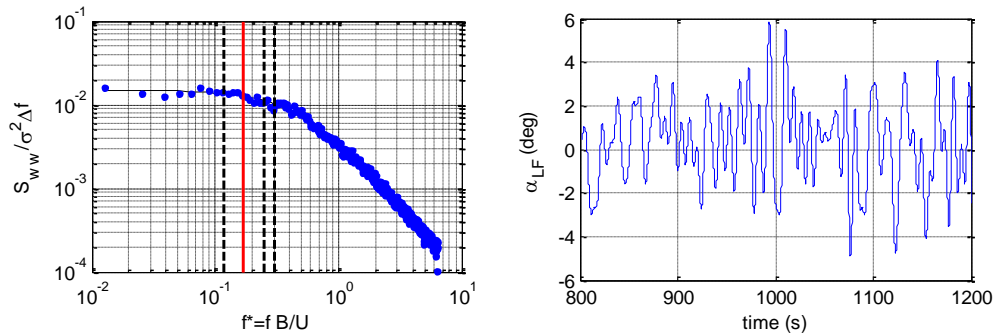


Figure 9: Left: Spectrum of w and threshold between LF and HF (red line); Right: a zoom of the time history of the LF angle of attack

Table 3: Comparison of results for different numerical models

Model	Linear	Rheological	Convolution
σ_y [m]	3.1	2.9	2.9
σ_z [m]	1.4	1.6	1.5
σ_θ [deg]	1.1	1.1	0.9
\max_y [m]	10.6	10	10.1
\max_z [m]	5.6	7.6	6.4
\max_θ [deg]	4.2	5.3	4.9

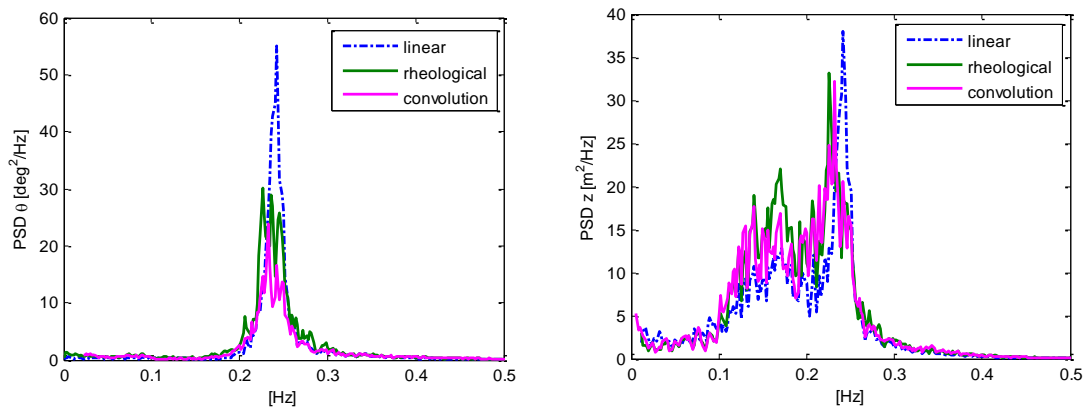


Figure 10: Comparison of the Power Spectral Densities of the deck response using linear and nonlinear approach: deck rotation θ (left) and vertical displacement z (right)

5 CONCLUSIONS

Two different realizations of the Band Superposition approach have been presented. A first one, based on a rheological model for aerodynamic forces results in an augmented dynamical system with time-varying parameters when coupled to the deck dynamics. The second one simulates the time histories of the aerodynamic forces by means of a time-varying convolution integral. In both cases, parameters are modulated by the low frequency response computed by a quasi-steady corrected theory.

Experimental results show that the Band superposition approach may represent correctly the non-linear characteristics of the aerodynamic forces, and both numerical models are suited. However, the rheological approach seems to be computationally more efficient.

The application of the BS approach to the simulation of a full-scale bridge allows one to evaluate the buffeting response of the structure including non-linearities. The effect of the spatial correlation of the turbulent wind fields still needs a deep investigation, together with and computationally more efficient implementation of the BS approach to a multi-section bridge.

References

- Chen, X., Kareem, A. (2001). Nonlinear response analysis of long-span bridges under turbulent winds. *J. Wind Eng. Ind. Aerodyn.* 89, 1335–1350.
- Chen, X., Kareem, A., (2003). Aeroelastic analysis of bridges: Effects of turbulence and aerodynamic nonlinearities. *Journal of Engineering Mechanics* 129, 885–895.
- Chen, X., Matsumoto, M., Kareem, A., (2000). Time domain flutter and buffeting response analysis of bridges. *Journal of Engineering Mechanics* 126, 7–16.
- Diana, G., Falco, M.; Bruni, S., Cigada, A., Larose, G., Damsgaard, A. & Collina, A. (1995) Comparisons between wind tunnel tests on a full aeroelastic model of the proposed bridge over Stretto di Messina and numerical results. *J. Wind Eng. Ind. Aerodyn.*, 54-55, 101 - 113
- Diana, G., Resta, F., Rocchi, D., (2008). A new numerical approach to reproduce bridge aerodynamic nonlinearities in time domain. *J. Wind Eng. Ind. Aerodyn.* 96, 1871 – 1884.
- Diana, G., Rocchi, D., Argentini, T., Muggiasca, S., (2010). Aerodynamic instability of a bridge deck section model: Linear and nonlinear approach to force modeling. *Journal of Wind Engineering and Industrial Aerodynamics* 98, 363–374.
- Diana, G., Rocchi, D., Argentini, T., (2013). An experimental validation of a band superposition model of the aerodynamic forces acting on multi-box deck sections. *Journal of Wind Engineering and Industrial Aerodynamics* 113, 40 – 58.